

Plasmons in Holographic Graphene

U. Gran,^a M. Tornso^a and T. Zingg^b

^a*Department of Physics, Division for Theoretical Physics, Chalmers University of Technology
SE-412 96 Göteborg, Sweden*

^b*Nordita, Stockholm University and KTH Royal Institute of Technology
Roslagstullsbacken 23, SE-106 91 Stockholm, Sweden
E-mail: ulf.gran@chalmers.se, marcus.tornso@chalmers.se,
zingg@nordita.org*

ABSTRACT: For strongly correlated systems, holography is an ideal framework for computing plasmon properties. We identify all these self-sourced modes in holographic Maxwell theories via a specific choice of boundary condition. This method's potential to improve holographic models of e.g. graphene is demonstrated by computing the 2D-plasmon dispersion, which naturally connects to regions in parameter space accessible to conventional methods.

Beyond that, this method also allows to compute the dynamical charge response of strange metals, which could be compared to experiments using (M-EELS).

Contents

1	Introduction	1
2	Physical Modes	2
3	Holographic Boundary Conditions for Physical Modes	3
4	Holographic Graphene as Codimension One Boundary Theory	5
5	Results	7
6	Conclusion	9

1 Introduction

Holography is a powerful framework for computing the response functions of strongly correlated matter to all orders in perturbation theory. Hereby, one has to distinguish between *screened* response functions, which, for example, describe the response to changes in the internal, screened electric field \mathcal{E} and the genuine, *physical* response functions [1] to the external electric displacement field \mathcal{D} . And it is the latter, which would be the quantity that is actually being tuned directly in an experimental setup. The relation between screened and physical response is encoded in the dielectric function ϵ , whose zeroes give the plasmon modes.

Thus, by analyzing ϵ we can both compare holographic models to experiments, as well as predict novel behavior of strongly correlated matter. Of particular interest is the little understood ‘strange-metal’ phase appearing e.g. above the critical temperature in high-temperature superconductors, and also in graphene in the form of the Dirac fluid. The dynamic charge response of strange metals, including plasmonic properties, has recently become experimentally accessible using the new method of momentum-resolved electron energy-loss spectroscopy (M-EELS) [2]. Note that we use the term “plasmon” rather loosely to describe propagating self-sourced plasma oscillations, even in the absence of long lived modes. In recent work [3], we demonstrated that one can describe plasmons holographically with a very specific choice of boundary conditions. In this paper, we generalize these findings further.

When considering linear response in holography, one generally obtains a set of coupled PDEs. Modes of the boundary theory correspond to specific solutions of these equations with a set of boundary conditions that would make the resulting boundary value problem over-determined. This is to be expected, however, since

modes, by definition, correspond to particular intrinsic properties of the system. The conditions at the horizon are determined by regularity of the solution, and are thus inviolable. At the boundary, conditions are related to the holographic dictionary, with different choices corresponding to different responses one wishes to study. What has been well-established is that Dirichlet conditions give quasi-normal modes (QNMs), which are identified with poles of the holographic Green function. The knowledge of only these modes, however, is not sufficient to characterize all electromagnetic properties, as they just give the response to a screened electric field \mathcal{E} , which is ‘internal’ to the system. To obtain the physical, response function, one needs to know the response to the, external, electric displacement field \mathcal{D} . In this work, we aim to fill this gap and, based on that, draw conclusions on what conditions holographic models need to satisfy in order to yield physically relevant results.

2 Physical Modes

Below, we summarize the notion of a ‘physical mode’ in the density-density response function – see e.g. [1]. In a medium, response to external electromagnetic fields is entirely described by Maxwell’s equations,

$$d\mathcal{F} = 0, \quad d \star \mathcal{W} = \star \mathcal{J}_{ext}. \quad (2.1)$$

The field strength \mathcal{F} and induction tensor \mathcal{W} are decomposed as,

$$\mathcal{F} = \mathcal{E} \wedge dt + \star^{-1}(\mathcal{B} \wedge dt), \quad (2.2)$$

$$\mathcal{W} = \mathcal{D} \wedge dt + \star^{-1}(\mathcal{H} \wedge dt). \quad (2.3)$$

Thus, \mathcal{W} describes the ‘external’ electric displacement field \mathcal{D} and magnetic field strength \mathcal{H} , which are sourced by an external current \mathcal{J}_{ext} . In contrast, \mathcal{F} describes the electric field strength \mathcal{E} and magnetic flux density \mathcal{B} inside the system, being the sums of the external fields and contributions from screening due to effects like polarization and magnetization in the material.

This distinction is relevant in order to decide which modes are to be considered ‘physical’. The Green function gives the response to the induced current,

$$\mathcal{J} = -\langle \rho \rangle dt + \mathbf{j} = \star^{-1} d \star (\mathcal{F} - \mathcal{W}), \quad (2.4)$$

when the gauge field \mathcal{A} is varied. This function encodes current-current correlations, and can be used to obtain conductivity or the ‘screened’ density-density response,

$$\sigma_{ij} = -\frac{\langle \mathbf{j}_i \mathbf{j}_j \rangle}{i\omega}, \quad \chi_{sc} = \langle \rho \rho \rangle. \quad (2.5)$$

And due to functional identities of the Green function, it is also straightforward to derive elementary identities like,

$$\chi_{sc} = \frac{k^2}{i\omega} \sigma_L, \quad (2.6)$$

where σ_L is the longitudinal conductivity. One has to keep in mind though, that these functions are ‘constructs’, as they describe the response to the screened fields \mathcal{F} , not the external fields \mathcal{W} . For an electric response, the relation between the screened and unscreened response is encoded in the dielectric function

$$\epsilon_{ij} = \frac{\partial \mathcal{D}_i}{\partial \mathcal{E}_j}. \quad (2.7)$$

In particular, for the physical density-density response,

$$\chi = \frac{\chi_{sc}}{\epsilon_L}. \quad (2.8)$$

Thus, a priori, physical modes, i.e. poles of the response function χ , would be given by the poles of χ_{sc} , as well as by the zeros of ϵ_L . However, due to Maxwell’s equations (2.1) there is a relation between the dielectric tensor and the conductivity,

$$\left(\epsilon - 1 + \frac{\sigma}{i\omega} \right) \cdot \mathcal{E} = \frac{\mathbf{k} \times \mathcal{M}}{\omega}. \quad (2.9)$$

In isotropic electromagnetic media in particular, this implies that poles of σ_L are also poles of ϵ_L , meaning that it is only the zeros of the latter that characterize the poles of the physical response χ .

3 Holographic Boundary Conditions for Physical Modes

In this section we will refine previous work [3] to illustrate how physical modes correspond to a specific choice of boundary conditions. In the following we will use the term ‘physical modes’ to refer to poles of physical response functions. That is, functions describing a response to an external, physical, source – in contrast to a response to the screened fields \mathcal{E} and \mathcal{B} . As argued in the last section, these physical modes correspond to the zeros of the longitudinal dielectric function ϵ_L . These correspond to modes for plasma oscillations inside the medium, so-called plasmons. It has been recently shown how to identify them holographically [3]. In that framework, these modes are again given by linear response in the electromagnetic sector, but one has to consider boundary conditions which are fundamentally different from Dirichlet conditions – as one would have when calculating QNMs, which would correspond to poles of the screened response χ_{sc} . This is because these modes characterize a situation where there are no external fields, i.e. $\mathcal{D} = 0$ and $\rho_{ext} = 0$, but there are effects like plasma oscillations, and thus $\mathcal{E} \neq 0$, in the interior of the material.

In the case of an isotropic system, there is only one transverse counterpart ϵ_T , and together with ϵ_L , they provide all necessary information to identify the physical modes of the system. We proceed by deriving the boundary conditions for corresponding bulk fields. Without loss of generality we impose $\delta \mathcal{A}_t \equiv \phi = 0$ and study a

harmonic perturbation with momentum in the x -direction, and y denoting any transverse direction. Then, after Fourier transforming, from Maxwell's equation (2.1) and the defining relation (2.4) in the absence of external fields, follows

$$\omega^2 \delta A_x + \delta \mathcal{J}_x = 0, \quad (3.1)$$

$$(\omega^2 - k^2) \delta A_y + \delta \mathcal{J}_y = 0. \quad (3.2)$$

These conditions can be turned into boundary conditions in the holographic dictionary, where we can relate the field strength on the boundary to the boundary value of the potential for the corresponding field in the bulk, as well as the current to the bulk induction tensor. Therefore, the explicit formulation is model-dependent, but in the class of Lagrangians usually studied in holography, the current is generally related to the normal derivative of the corresponding potential at the boundary, such that,

$$\omega^2 \delta A_x + p_L \delta A'_x = 0, \quad (3.3)$$

$$(\omega^2 - k^2) \delta A_y + p_T \delta A'_y = 0. \quad (3.4)$$

These provide a unified description of all self-sourced solutions to holographic Maxwell theories. The functions $p_{L/T}$ are determined by the specific bulk theory at hand and the holographic dictionary [3]. They are generally bounded, but may depend on ω and k . In the case of a standard Maxwell action in the bulk, p is constant. The type of mixed boundary conditions we arrive at are related to a double trace deformation in the QFT [4, 5], corresponding to the RPA form of the Green function [6]. Therefore, our approach is consistent with conventional CMT and in fact quite natural for computing the dielectric function.

It is also straightforward to reformulate the boundary conditions in term of the dielectric function. This essentially follows from basic definitions and the relation (2.9), as well as noting that in the absence of external fields we have $\mathcal{M} = \mathcal{B}$. Then, a bit of algebra reveals that (3.1) and (3.2) are nothing else but

$$\epsilon_L(k, \omega) = 0, \quad \epsilon_T(k, \omega) = 0. \quad (3.5)$$

The first one, in accordance with the nomenclature in [3], we will refer to as the plasmon condition, and the modes satisfying it as plasmons. The second one, i.e. the counterpart in the transverse direction, are transverse symmetric waves [1] involving transverse current fluctuations.

We emphasize that the modes corresponding to (3.3) and (3.4) are complementary to QNMs. The latter correspond to poles of the Green function for internal correlators, the former being necessary to relate aforementioned to external, physical, quantities that can actually be accessed via experiment. Thus, identifying all physical modes is a crucial step to relate holographic results to actual data and, for the holographic Maxwell theories we consider, all physical modes correspond to (3.3) and (3.4), as explained above.

4 Holographic Graphene as Codimension One Boundary Theory

All electromagnetic phenomena can be described through the field strength \mathcal{F} and the induction tensor \mathcal{W} . While it has been known for a while how to identify the former in the boundary theory, the correspondence for the latter seems to have gone unmentioned until recently [3]. In the following we will examine consequences of this identification with regard to codimension one systems, like graphene. For a different holographic bottom-up model of graphene see [7].

Holography has been established as an effective description of strongly correlated systems. However, while the strength of interaction is large in these systems, one does not wish to change the fundamental nature of the interaction, respectively test charges, itself. And the latter is intricately connected with the dimension in which particles interact, as creation and annihilation operators are determined as distribution-valued operators for point-like sources. This becomes relevant in systems like graphene, certain high- T_c superconductors and other compound materials, where charge carriers move in layers – or even edges, in some cases. I.e. positioning is confined to a lower number of dimensions, but the charge carriers are, in essence, still subject to interactions determined by the ‘ $1/r$ ’ Coulomb potential in three spatial dimensions – in contrast to, e.g., the ‘ $\ln r$ ’ potential in two dimensions. In a proper description of such a material, this feature must therefore also be incorporated into an effective model. Meaning that while the system one wishes to study is effectively $(2+1)$ -dimensional, one has still to keep in mind that it is composed of particles whose electromagnetic interaction is determined by Maxwell’s equations in $(3+1)$ -dimensions.

From a holographic perspective, this requires to incorporate a mechanism that keeps particles ‘in place’. In a top-down construction, this is usually achieved via embedding D-branes, which is also how aspects of graphene and related systems were holographically modeled previously [8–13], and is illustrated in figure 1. This description, however, will create some difficulties from a practical standpoint. As pointed out in previous work [3], gravitational back-reaction seems crucial to determine material properties like plasmon excitations. For D-branes, however, going beyond a probe limit – in which back-reaction is neglected – is a rather difficult task where, in general, no efficient computational methods are at hand.

Nevertheless, we will present a toy-model that incorporates all the necessary features to demonstrate that the interplay of confinement to a lower-dimensional subspace and gravitational back-reaction in a holographic model will combine to provide physically realistic results. The important point to keep in mind is that it is not so much the details of the gravitational interaction with the brane that is relevant, rather that there is some mediating interaction with the background. Thus, as a proxy, consider the gravitational interaction ‘projected’ onto the brane – which

is sufficient, since we are only interested in studying phenomena due to particles that are, ultimately, constrained to not being able to move beyond the dimensions in which the brane extends. The crucial ingredient will be the appropriate choice of the function p_L in (3.3) for the condition on the boundary at asymptotic infinity, such that it properly reflects the feature of a codimension one system, where the gauge potential can permeate one dimension more than the induced current. To

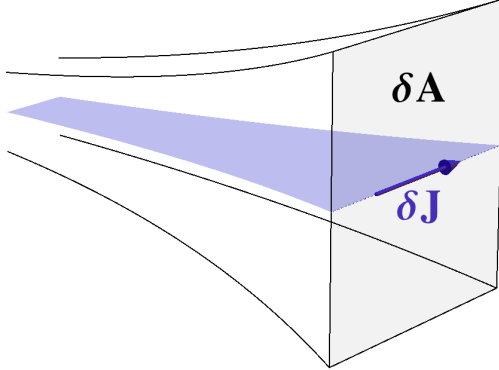


Figure 1. Schematics of a holographic setup for a physically realistic model for graphene. While the induced current δJ on the boundary is confined to $2 + 1$ dimensions, the boundary potential δA lives in $3 + 1$ dimensions. Therefore, a realistic holographic setup would require a brane-construction that keeps particles in place and electromagnetic phenomena are described by the bulk physics projected onto the brane.

derive this condition, consider first an ordinary $(3 + 1)$ -dimensional system. The longitudinal boundary condition can be derived rather straightforwardly from the Coulomb potential. For simplicity, we work in Coulomb gauge $A_t = \phi$ and $A_x = 0$. In the absence of external sources, a perturbation of the internal charge density $\delta\rho$ must be related to a change in the potential,

$$\delta\phi(t, \mathbf{r}) = \int d^3r' \frac{\delta\rho(t, \mathbf{r}')}{4\pi|\mathbf{r} - \mathbf{r}'|}. \quad (4.1)$$

Before proceeding, we emphasize that even though this seems like an instantaneous Coulomb interaction, this is the fully relativistic result following from a retarded interaction. The apparent conundrum is simply due to the fact that the choice of Coulomb gauge makes the interaction just look instantaneous, while it, of course, still preserves causality – see e.g. [14].

At any rate, after Fourier-transforming (4.1),

$$\delta\phi(\omega, \mathbf{k}) = \frac{1}{\mathbf{k}^2} \delta\rho(\omega, \mathbf{k}), \quad (4.2)$$

which, via a gauge change and the continuity equation, corresponds to exactly (3.1). However, if the charges are confined to a plane $z = 0$, the integral (4.1) has to be

adjusted with a delta function in the z -direction, which modifies (3.1) to

$$\omega^2 \delta A_x + \frac{|k|}{2} \delta J_x = 0, \quad \delta A_t = 0. \quad (4.3)$$

This suggests that, for a toy model, one can compensate the lack of an additional dimension for the fields by changing p_L of (3.3) to include an additional factor $|k|/2$. We will show below that this is indeed the crucial ingredient to find a physically accurate response.

5 Results

The model described above is, up to the change in the boundary condition, identical regarding conventions and setup to [3]. The longitudinal result is presented in figures 2 and 3. As expected, for a non-zero charge, the dispersion relation is $\omega \propto \sqrt{k}$ for small k , and $\omega \approx k$, i.e. the dispersion of a free mode, for large k . The small k behavior can in fact be derived analytically to be

$$\omega(k) = \sqrt{\frac{2Q^2}{6 + 3Q^2}} \sqrt{k} - i \left(\frac{6 - Q^2}{12 + 6Q^2} \right)^2 k + \dots \quad (5.1)$$

Furthermore, the consistency of the model can be checked by considering that it must be subject to certain sum rules. And, within numerical precision, we indeed can verify that $\lim_{k \rightarrow 0} \int_0^\infty d\omega \text{Im} [\epsilon(\omega, k)^{-1}/\omega] = -\pi/2$, as required, c.f. [15] for details. The apparent divergence at $k \rightarrow 0$, is expected for charges perfectly confined to a plane. A less perfect confinement, which in an ideal model would correspond to smearing of the branes, would introduce a cut-off at small enough k with an instead linear dispersion. The dispersion is thus not to confuse with that of surface plasmons at an *interface*, where charges are not strictly confined to a plane.

Beyond that, we can reach regions of parameter space which has only recently become accessible to experiments, such as $\mu \approx T$ relevant for the Dirac fluid in graphene [16–18]. The extreme case $\mu/T = 0$ is possible to observe for truly neutral media (such as He-3), and our result for this case can be seen in figure 2 and 3. Here, we can note that for small k there is the zero sound mode $\omega \approx k/\sqrt{2}$ and the linear $\omega \approx k$ mode for large k . This is in accordance with the expectation that the plasmon mode of charged systems turns into the zero sound mode for neutral ones. Since we can access the finite $\mu \ll T$ region, we can also predict how this happens, with the result being that there are three regions. For small k , there is the plasmon $\omega \propto \sqrt{k}$, for intermediate k , there is zero sound $\omega \approx k/\sqrt{2}$ and for large k , there is the free linear mode $\omega \approx k$. One way to present these different regions is by plotting the derivative of the logarithms, shown in figure 4, with the regions mentioned above as I, II and III in the figure.

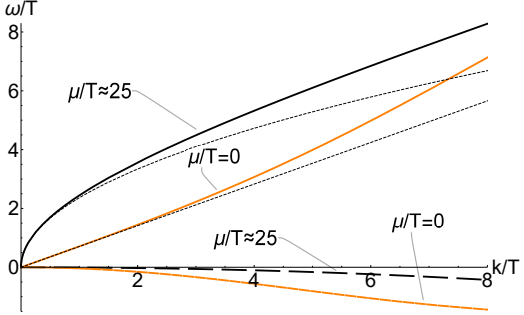


Figure 2. The lowest $\epsilon = 0$ mode for the RN background at $\mu/T = 0$ and $\mu/T \approx 25$ with $p = k/2$. Imaginary parts are negative and dashed. The thin dotted black lines are the expected asymptotes $\omega = k/\sqrt{2}$ and $\omega \propto \sqrt{k}$ respectively.

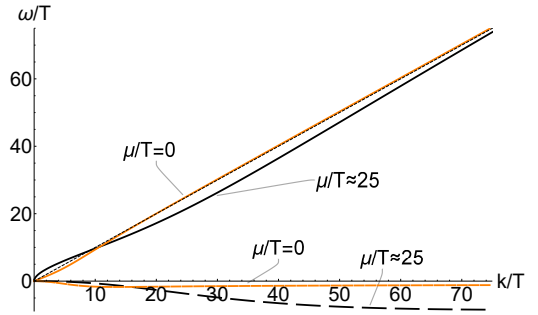


Figure 3. The lowest $\epsilon = 0$ mode for the RN background at $\mu/T = 0$ and $\mu/T \approx 25$ with $p = k/2$. Imaginary parts are negative and dashed. The thin dotted black line (mostly inside the orange line) is the expected asymptote $\omega = k$.

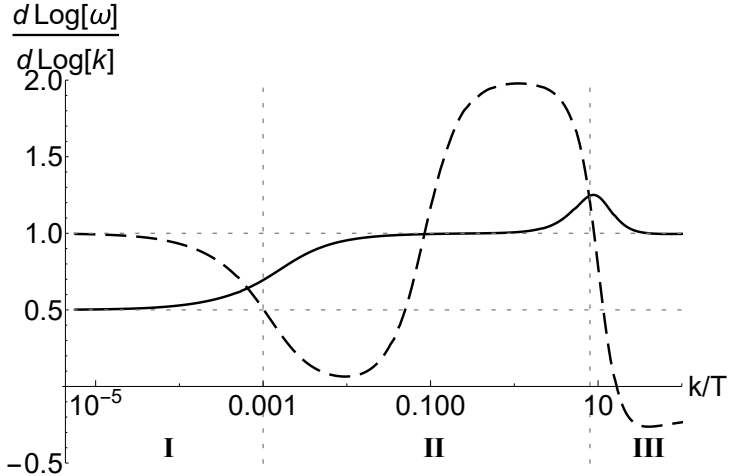


Figure 4. The derivatives $\frac{d \log \Re \omega}{d k}$ (solid), respectively $\frac{d \log -\Im \omega}{d k}$ (dashed) for the lowest $\epsilon = 0$ mode at $\mu/T \approx 0.08$ with $p = k/2$. Note how $\omega \propto \sqrt{k} + i\Gamma k \rightarrow k + i\Gamma k^2 \rightarrow k$.

In particular, note the significant difference in physics between the two linear modes in figure 2 and 3. The zero sound mode depends on changes in the Fermi surface, and is thus dimension dependent (hence the factor $1/\sqrt{2}$) and increasingly unstable when increasing k . The free mode, being dimension independent, has speed 1, in units where $c = 1$, and an imaginary part largely unaffected by increasing k .

It is also worth stressing that the dispersion we compute holographically agrees with the results from conventional condensed matter approaches for the regions of configuration space where comparisons can be made. In particular, in the small k region where $\omega \propto \sqrt{k}$, in addition to matching the real part of the dispersion also the linear dependence of the imaginary part of ω on k , c.f. figure 4, matches recent

computations for this ‘‘collisionless plasmon’’ part of the configuration space [19]. Also, for small k the results match hydrodynamic¹ results [20], but note however that since a mechanism for impurity scatterings is not explicitly included in our model, a proper hydrodynamic region is not to be expected.

6 Conclusion

In this paper we analyze the conditions all physical modes in holography must satisfy, building on the results of [3]. We find that for isotropic systems there are boundary conditions that translate the necessary features from the boundary theory into the bulk, (3.3) and (3.4) for longitudinal and transverse modes, respectively. We also point out that, in the case of holographic Maxwell theories, poles of the screened correlator χ_{sc} , corresponding to QNMs, are not physical modes.

We then demonstrate that this method of relating the physical set-up in the boundary theory to the boundary conditions on the equations of motion in the bulk is not only instructive and intuitive, but also a powerful tool when regarding other types of Maxwell theories, such as codimension one materials. For such, we obtain the very characteristic $\omega \propto \sqrt{k}$ dispersion for small k , using the simple planar AdS₄-RN model. This has previously been impossible both in bottom-up systems, since the mode is heavily dimension dependent, and in top-down systems, since the mode also requires a dynamically back-reacted metric.

The use of mixed boundary conditions that are tailored to the boundary theory opens up a wide range of possible follow-up studies to previous work, as they can be applied to previously examined bulk theories. Especially interesting are models that include a physically more realistic mechanism for dynamical polarization, and back-reacted top-down models that have a bulk theory that better aligns with the boundary theory in codimension one systems while still keeping backreacted gravity effects in the bulk.

Acknowledgments

We would like to thank Johanna Erdmenger, Bert Hecht and Tobias Wenger for valuable discussions. This work is supported by the Swedish Research Council.

¹For non-zero values of the intrinsic electrical conductivity σ_Q , which is the generic case for the hydrodynamic limit of holographic models. Other common names for σ_Q are the quantum critical or incoherent conductivity.

References

- [1] D. Pines and P. Nozières, *The Theory of Quantum Liquids*. W.A. Benjamin Inc., 1966.
- [2] M. Mitrano, A. A. Husain, S. Vig, A. Kogar, M. S. Rak, S. I. Rubeck, J. Schmalian, B. Uchoa, J. Schneeloch, R. Zhong, G. D. Gu, and P. Abbamonte, *Singular density fluctuations in the strange metal phase of a copper-oxide superconductor*, [arXiv:1708.0192](https://arxiv.org/abs/1708.0192).
- [3] M. Aronsson, U. Gran, and T. Zingg, *Holographic Plasmons*, [arXiv:1712.0567](https://arxiv.org/abs/1712.0567).
- [4] E. Witten, *Multitrace operators, boundary conditions, and AdS / CFT correspondence*, [hep-th/0112258](https://arxiv.org/abs/hep-th/0112258).
- [5] W. Mueck, *An Improved correspondence formula for AdS / CFT with multitrace operators*, *Phys. Lett.* **B531** (2002) 301–304, [[hep-th/0201100](https://arxiv.org/abs/hep-th/0201100)].
- [6] J. Zaanen, Y.-W. Sun, Y. Liu, and K. Schalm, *Holographic Duality in Condensed Matter Physics*. Cambridge Univ. Press, 2015.
- [7] Y. Seo, G. Song, P. Kim, S. Sachdev, and S.-J. Sin, *Holography of the Dirac Fluid in Graphene with two currents*, *Phys. Rev. Lett.* **118** (2017), no. 3 036601, [[arXiv:1609.0358](https://arxiv.org/abs/1609.0358)].
- [8] S.-J. Rey, *String theory on thin semiconductors: Holographic realization of Fermi points and surfaces*, *Prog. Theor. Phys. Suppl.* **177** (2009) 128–142, [[arXiv:0911.5295](https://arxiv.org/abs/0911.5295)].
- [9] R. C. Myers and M. C. Wapler, *Transport Properties of Holographic Defects*, *JHEP* **12** (2008) 115, [[arXiv:0811.0480](https://arxiv.org/abs/0811.0480)].
- [10] O. Bergman, N. Jokela, G. Lifschytz, and M. Lippert, *Quantum Hall Effect in a Holographic Model*, *JHEP* **10** (2010) 063, [[arXiv:1003.4965](https://arxiv.org/abs/1003.4965)].
- [11] J. L. Davis, H. Omid, and G. W. Semenoff, *Holographic Fermionic Fixed Points in d=3*, *JHEP* **09** (2011) 124, [[arXiv:1107.4397](https://arxiv.org/abs/1107.4397)].
- [12] H. Omid and G. W. Semenoff, *D3-D7 Holographic dual of a perturbed 3D CFT*, *Phys. Rev.* **D88** (2013), no. 2 026006, [[arXiv:1208.5176](https://arxiv.org/abs/1208.5176)].
- [13] G. W. Semenoff, *Engineering holographic graphene*, *AIP Conf. Proc.* **1483** (2012) 305–329.
- [14] J. D. Jackson, *From Lorenz to Coulomb and other explicit gauge transformations*, *Am. J. Phys.* **70** (2002) 917–928, [[physics/0204034](https://arxiv.org/abs/physics/0204034)].
- [15] G. Mahan, *Many-Particle Physics*. Physics of Solids and Liquids. Springer US, 2000.
- [16] D. A. Bandurin, I. Torre, R. K. Kumar, M. Ben Shalom, A. Tomadin, A. Principi, G. H. Auton, E. Khestanova, K. S. Novoselov, I. V. Grigorieva, L. A. Ponomarenko, A. K. Geim, and M. Polini, *Negative local resistance caused by viscous electron backflow in graphene*, *Science* **351** (Mar., 2016) 1055–1058, [[arXiv:1509.0416](https://arxiv.org/abs/1509.0416)].

- [17] J. Crossno, J. K. Shi, K. Wang, X. Liu, A. Harzheim, A. Lucas, S. Sachdev, P. Kim, T. Taniguchi, K. Watanabe, T. A. Ohki, and K. C. Fong, *Observation of the Dirac fluid and the breakdown of the Wiedemann-Franz law in graphene*, *Science* **351** (Mar., 2016) 1058–1061, [[arXiv:1509.0471](https://arxiv.org/abs/1509.0471)].
- [18] P. J. W. Moll, P. Kushwaha, N. Nandi, B. Schmidt, and A. P. Mackenzie, *Evidence for hydrodynamic electron flow in $PdCoO_2$* , *Science* **351** (Mar., 2016) 1061–1064, [[arXiv:1509.0569](https://arxiv.org/abs/1509.0569)].
- [19] A. Lucas and S. Das Sarma, *Electronic sound modes and plasmons in hydrodynamic two-dimensional metals*, [arXiv:1801.0149](https://arxiv.org/abs/1801.0149).
- [20] A. Lucas and K. C. Fong, *Hydrodynamics of electrons in graphene*, *J. Phys. Condens. Matter* **30** (2018) 053001, [[arXiv:1710.0842](https://arxiv.org/abs/1710.0842)].